*Int. J. Multiphase Flow* Vol. 16, No. 1, pp. 19–34, 1990
Printed in Great Britain

0301-9322/90 $3.00 + 0.00
Pergamon Press plc

# PARTICLE LAGRANGIAN SIMULATION IN TURBULENT FLOWS

A. BERLEMONT, P. DESJONQUERES and G. GOUESBET
Laboratoire d'Energétique des Systèmes et Procédés, UA CNRS 230, INSA, B.P. 08, Place Emile Blondel, 76131 Mont-Saint-Aignan, Cédex, France

(*Received* 25 *June* 1988; *in revised form* 27 *April* 1989)

**Abstract**—A Lagrangian approach is used to describe particle dispersion in turbulent flows. Fluid particle trajectories are simulated with the aid of a correlation matrix evolving along the particle trajectory. Discrete particles are tracked in a given turbulent field taking into account crossing-trajectory effects, and the influence of the particles on the flow characteristics is deduced from momentum and energy exchanges between both phases. Comparisons of the simulations are given for both experimental and theoretical results for fluid particle diffusion problems. Particle dispersion predictions are presented for grid turbulence experiments, and for three two-phase turbulent round jets, from different authors. Predictions compared favourably with experimental results.

*Key Words:* turbulence, two-phase flows, Lagrangian simulation, dispersed flows, turbulent diffusion

## 1. INTRODUCTION

In the Universe, fluids are nearly everywhere, and they almost invariably contain particles. Applications of multiphase flow theories are therefore very wide and potentially infinite. Numerous models have been designed to study various situations, such as particle dispersion or transport, bubbly flows, slug and annular flows, and transitions between all these regimes.

This paper is devoted to particle dispersion in turbulent flows, which has become a major domain of research attracting increasing interest and with challenging fundamental aspects. Various applications are concerned, more particularly in geophysical systems, or in laboratory and industrial applications: pulverized coal or droplet flames, diesel engines or some rocket exhausts with applications to guidance control and radar detection...

Theoretical studies of particle dispersion can be developed either by a Eulerian approach or a Lagrangian approach. The Eulerian approach is based on the assumption that two continuous fields are present, and transport equations are solved for both phases (Abbas *et al.* 1980; Reeks 1977; Durst *et al.* 1984; Elghobashi *et al.* 1984); this approach has also been developed previously by the authors (Gouesbet & Berlemont 1981; Gouesbet *et al.* 1984; Desjonqueres *et al.* 1986; Picart *et al.* 1986).

In the Lagrangian approach, a number of particle trajectories are simulated, in a given turbulence field, i.e. the particles are considered individually. Statistical computations then lead to mean values which characterize the particle behaviour. Most of the papers on the topic are based on the "eddy lifetime" concept (e.g. Gosman & Ioannides 1981; Shuen *et al.* 1985; Durst *et al.* 1984). In Ormancey & Martinon (1984), another method is developed, namely the influence of the turbulence field on discrete particles moving in flows is mostly represented by following simultaneously a discrete particle and a fluid particle and, as will be described, by taking into account the instantaneous properties of the fluid in the construction of a discrete particle trajectory, at each time step. This new scheme is also used in the present paper.

The particle trajectory simulation is different, depending on whether a fluid or a discrete particle is followed. For a fluid particle, its instantaneous velocity can be determined knowing the mean velocity, deduced from a $(K-\epsilon)$ model, and the fluctuating velocity correlations from algebraic relations deduced from a second-order closure scheme (Gouesbet & Berlemont 1981; Berlemont *et al.* 1986).

Our Lagrangian technique is, however, quite new since a correlation matrix is used in the random process, which simulates the Lagrangian time correlations along the whole particle trajectory. The eddy lifetime method implicitly produces a linear decrease in the Lagrangian time correlation, while

the Ormancey & Martinon (1984) method implicitly produces an exponential decrease. Our correlation matrix technique permits us to explicitly introduce any shape of the Lagrangian time correlation function. Linear and exponential decreases can then be recovered as special cases of our much more general formulation.

For a discrete particle, forces acting on the particle are expressed through the Riley (1971) equation of motion and corrected with coefficients from Clift *et al.* (1978) and Odar & Hamilton (1964) for non-small particle Reynolds numbers and acceleration numbers. The instantaneous fluid velocity at the discrete particle location is obtained by use of Eulerian correlations in a characteristic correlation domain.

The particle behaviour is mostly determined by the nature of the particle and the effects of the turbulence on their motion. But, in many industrial processes, the particle/fluid mass loading is large enough to modify the flow itself. These modifications can occur locally, i.e. just around the particle, whatever the flow, but sometimes they can change the whole turbulence field characteristics. We therefore have to deal with a two-way coupling turbulence/particle, which will be presented here also, using source terms for momentum and energy exchanges between both phases.

This paper reports on the computer program PALAS (PArticle LAgrangian Simulation) for the prediction of particle dispersion in turbulent flows within the framework of our Lagrangian approach. Fluid particle trajectory, discrete particle trajectory and particle/turbulence interactions are successively discussed and comparisons with experimental and theoretical results are given.

## 2. FLUID PARTICLE TRAJECTORY

The first step in the Lagrangian approach under study is to simulate a fluid particle trajectory. The basic equation to integrate is quite simple:

$$x_i(t + \Delta t) = x_i(t) + U_i \Delta t, \qquad [1]$$

where $x_i(t)$ represents the location of the particle at the time $t$, $U_i$ is its instantaneous velocity and $\Delta t$ is the time step. The instantaneous velocity reads as the sum of the mean velocity $\overline{U}_i$ and a fluctuating velocity $u_i$.

The mean velocity is known either from experimental data or from computational predictions of the considered flow. The variances of the fluctuating velocities, and more generally the Reynolds stress tensor components, are also obtained in the same way (in our case, they are estimated from algebraic relations deduced from a second-order closure scheme). Hence, the main problem is to evaluate the fluctuating velocities $u_i$, from the knowledge of the covariances $\overline{u_i u_j}$. As a first step, we assume that the pdf of the fluctuating velocity field is Gaussian. Then the statistical properties of the field are determined by Lagrangian correlations.

A simple way to take into account such correlations is to assume an exponential form for the correlation coefficient:

$$R_{fL}(\tau) = \exp\left(-\frac{\tau}{\tau_L}\right), \qquad [2]$$

where $\tau_L$ is the Lagrangian integral time scale.

Such a simulation is easily obtained with the use of a Poisson scheme (Ormancey & Martinon 1984). A similar method has been frequently used by different authors, in which the Lagrangian correlation is replaced by an "eddy lifetime", depending on $\tau_L$ and on the transit time of the particle in a given cell (Gosman & Ioannides 1981; Shuen *et al.* 1985; Durst *et al.* 1984), but that leads to a linear function for the correlation—quite a rough approximation.

However, following Hinze (1975, p. 398), it can be shown from considerations about the non-existence of an integral time scale for accelerations, that a more satisfactory relation for the Lagrangian correlation function $R_{fL}(\tau)$ is obtained by introducing negative loops in the expression.

The Eulerian code DISCO, previously developed in Rouen, involves a Frenkiel (1948) family of Lagrangian correlation functions, expressed by

$$R_{fL}(\tau) = \exp\left[\frac{-\tau}{(m^2+1)\tau_L}\right]\cos\left[\frac{m\tau}{(m^2+1)\tau_L}\right], \qquad [3]$$

where $m$ is a loop parameter, linked to the number and the importance of the negative parts in the correlation. Note that a value of zero for this parameter leads to an exponential form for the correlation.

The value $m = 1$ has given good agreements with various experimental situations (grid turbulence, pipe flow . . .) when used in the Eulerian code, and we thus decided to implement such a correlation function when elaborating the Lagrangian approach. However, this particular choice of $R_{fL}$-shape is by no means conceptually essential to our approach, although it is important for the quality of the result (figure 2, for instance).

Also more sophisticated turbulence models might permit an *a priori* computation of the function $R_{fL}$, which then could be included in our approach without any other modification to our Lagrangian scheme. More generally, this Lagrangian approach is not dependent on the specific turbulence model used in the present paper. It means that any method which generates the fluctuating velocity field can be substituted for our choice of turbulence. However, note that a $(K$–$\epsilon)$ model supplemented with algebraic relations for the Reynolds stress tensor and Frenkiel functions for $R_{fL}$, provides high-quality results in a reasonable CPU time.

### *2.1. The One-dimensional Formalism*

Let $u_x(n\Delta t)$ be the value of the fluctuating velocity at the time $n\Delta t$. Equation [1] can be integrated, and a trajectory constructed, if we can define a vector **U** of correlated random variables:

$$\mathbf{U} = (u_x(0), u_x(\Delta t), u_x(2\Delta t), \ldots, u_x(i\Delta t), \ldots, u_x(n\Delta t)), \qquad [4]$$

where $n$ represents the number of time steps needed for the considered trajectory; $n$ is either constant, when dispersion is computed as a function of time, or a variable depending on the velocity of the particle, when the dispersion is computed as a function of the distance from the injector in a non-uniform flow. The components of **U** have to comply with the given Lagrangian correlation function and the Gaussian pdf.

The mathematical process to generate **U** is as follows:

—We first define a vector **Y** $(y_i)$ of uncorrelated variables with a Gaussian distribution satisfying

$$\overline{y_i^2} = 1; \quad \overline{y_i} = 0; \quad \overline{y_i y_j} = 0 \qquad (i \neq j). \qquad [5]$$

—**U** and **Y** are related through a matrix $B\,(b_{ij})$:

$$\mathbf{U} = B\mathbf{Y}. \qquad [6]$$

From [5] and [6], the Lagrangian correlations read:

$$\overline{u(i\Delta t)u(j\Delta t)} = \sum_k b_{ik} b_{jk}. \qquad [7]$$

Defining the correlation matrix $A\,(a_{ij})$,

$$a_{ij} = \overline{u(i\Delta t)u(j\Delta t)}, \qquad [8]$$

the matrix $B$ is then determined by ([7] and [8])

$$A = B\,B^{\mathrm{T}}, \qquad [9]$$

where $B^{\mathrm{T}}$ is the transposed matrix of $B$.

We thus obtain a Cholesky factorization of the matrix $A$. The whole process is mathematically valid when $A$ is a symmetric, positive-definite matrix. Choosing positive elements $b_{ii}$ of $B$, we use the Cholesky algorithm according to the following relations (Ciarlet 1982):

$$b_{11} = \sqrt{a_{11}}, \qquad [10a]$$

$$b_{i1} = \frac{a_{i1}}{b_{11}}, \qquad [10b]$$

$$b_{ij} = \frac{a_{ij} - \sum_{k=1}^{j-1} b_{ik} b_{jk}}{b_{jj}} \qquad (i \neq j < 1). \tag{10c}$$

and

$$b_{ii} = \sqrt{a_{ii} - \sum_{k=1}^{i-1} b_{ik}^2} \qquad (i \neq 1). \tag{10d}$$

Let us note, when looking at these relations, that the $i$th line of $B$ depends only on the $i$th line of $A$ and on the previously computed elements of $B$ ($b_{jk}; j < i$). This allows us to compute the matrix $B$ and, consequently, the fluctuating velocities $u_i$, step by step. That means that we really build a fluid particle trajectory, as every fluctuating velocity $u_i$ depends on all the previously-encountered velocities, for a given particle.

### 2.2. The Two-dimensional Formalism

For two-dimensional flows, which are considered here, we need at each time step to estimate $u_x(k\Delta t)$ and $u_y(k\Delta t)$, as the particle trajectory is determined by a vector, defined by

$$\mathbf{U} = (u_x(0), u_y(0), u_x(\Delta t),\ u_y(\Delta t), \ldots, u_x(i\Delta t), u_y(i\Delta t), \ldots). \tag{11}$$

The correlation matrix $A$ in this case involves three kinds of elements (see the appendix):

(i) $\overline{u_x u_x(k\Delta t)}$, $\overline{u_y u_y(k\Delta t)}$ and $\overline{u_x u_y(k\Delta t)}$, which are deduced from the Reynolds stress tensor predictions in the turbulence part of the code.

(ii) $\overline{u_x(i\Delta t) u_x(j\Delta t)}$ and $\overline{u_y(i\Delta t) u_y(j\Delta t)}$, which are temporal autocorrelations expressed by a Frenkiel function.

(iii) $\overline{u_x(i\Delta t) u_y(j\Delta t)}$ which are temporal cross-correlations also expressed with the aid of the Frenkiel family of correlation functions.

Note that these terms are linked to the non-diagonal terms of the dispersion tensor used in the Eulerian approach (Picart 1984), which have been shown to be negligible in most cases. However, they are included in the Lagrangian approach as they are necessary for the Cholesky factorization.

### 2.3. Simplifications

The method described here is simplified as follows.

(i) A reduced matrix $R$, instead of $A$, is used, defined by

$$r_{ij} = \frac{\overline{u(i\Delta t) u(j\Delta t)}}{\sqrt{\overline{u^2(i\Delta t)}} \sqrt{\overline{u^2(j\Delta t)}}} \tag{12}$$

or, with the Frenkiel family of correlation functions,

$$r_{ij} = \exp\left[\frac{-|j-i|\Delta t}{(m^2+1)\tau_L}\right] \cos\left[\frac{m|j-i|\Delta t}{(m^2+1)\tau_L}\right]. \tag{13}$$

This scheme enables us to reduce the computing time.

(ii) The matrix size can be physically limited when the diffusion time is larger than 10 times the Lagrangian integral time scale, since the correlation is nearly equal to zero. The average number of elements for one-dimensional problems in the matrix is thus of the order of $10\tau_L/\Delta t$.

(iii) The Cholesky scheme is carried out step by step, without storage of the whole matrix.

(iv) The most important simplification is that a larger time step $\Delta t$ can be chosen with our method than with the Poisson process or the "eddy lifetime" scheme. For instance, in the case of diffusion from a point source (described in next section), a similar precision is reached with $\Delta t = 0.2\tau_L$ with the correlation matrix, compared with a time step of the order of $0.01\tau_L$ for the Poisson scheme.

### 2.4. Comparisons with Theoretical Results

Numerical computations have been carried out to check the validity of the method (Desjonqueres 1987), but an important part in the validation of the method is to compare numerical results with analytical solutions.

In the particular case of homogeneous, isotropic turbulence, Hinze (1975) writes the probability of a fluid particle to be located at a given point, as follows:

$$C(x,r) = \frac{S}{4\pi\epsilon_f|x|}\exp\left(\frac{-U_x r^2}{4\epsilon_f|x|}\right), \qquad [14]$$

where $x$ is the distance from the source (for diffusion from a continuous source of constant strength $S$, far away from the origin and near the axis), $r$ is the radial coordinate, $\epsilon_f$ is the diffusion coefficient and $U_x$ the mean velocity in the $x$-direction.

Figure 1 shows concentration profiles, for a distance $x = 500$ cm from the source vs the radial location. We used $U_x = 655$ cm/s, $U_r = 0$, $\overline{u_x^2} = \overline{u_r^2} = 171$ cm$^2$/s$^2$ and $\epsilon_f = 15.6$ cm$^2$/s; i.e. $\tau_L = 91$ ms ($\epsilon_f = \overline{u^2}\tau_L$ for long diffusion times).

The comparisons in figure 1 are between the theoretical results, simulations with our scheme with negative loops in the correlation ($m = 1$) and simulations with $m = 0$, i.e. with the Poisson process and an exponential form for the correlation. The very good agreement between the simulations and theoretical results confirms the validity of our approach. These results are also seemingly in favour of the value $m = 1$. However, in Lagrangian simulations, the observed differences between $m = 0$ and $m = 1$ are essentially due to transient evolutions of the time-dependent diffusion coefficient $\epsilon(t)$ before it reaches its asymptotic value, while in [14] this coefficient is constant. Consequently, the better agreement for $m = 1$ should not be stated too seriously. The next section will provide us with a non-ambiguous confirmation of the quality of the value $m = 1$.

### *2.5. Comparisons with Experimental Results*

To justify our choice between $m = 0$ and $m = 1$, let us consider the case of fluid particle dispersion in a turbulent pipe flow. The experiments have been described by Taylor & Middleman (1974) and the results here concern the mean square displacement $\overline{Y^2}$ of a tracer in a turbulent pipe flow of water, for a Reynolds number of 35,000, with a mean velocity on the axis of 85 cm/s and a pipe diameter of 5.08 cm. The Lagrangian integral time scale is 80 ms for a turbulence intensity of 3.2% on the centreline. The simulations are performed with the assumption that the turbulence is homogeneous along the particle trajectory, and that the flow is fully developed. Experimental data are used for turbulence quantities, in order to reduce the discrepancies coming from turbulence predictions.

The results are presented in figure 2 for the mean square displacement $\overline{Y^2}$ vs the diffusion time $t$. Experiments are compared with:

(i) the Lagrangian approach PALAS for $m = 1$ (with the correlation matrix);
(ii) the Lagrangian approach for $m = 0$ (Poisson process);
(iii) the Eulerian approach DISCO developed previously (Picart *et al.* 1986).

Note that the case $m = 0$ leads to under-predicted values for $\overline{Y^2}$, and that a very satisfactory agreement is observed between the experiments and "PALAS, $m = 1$", and also between PALAS and DISCO.

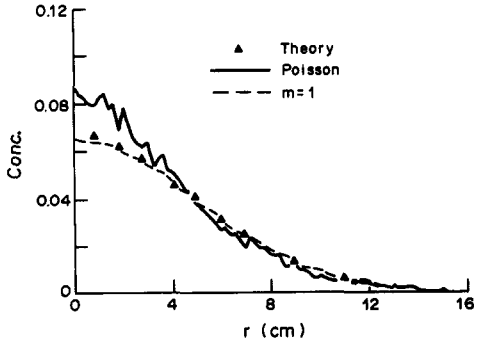


Figure 1. Diffusion from a point source in homogeneous, isotropic turbulence (Hinze 1975).

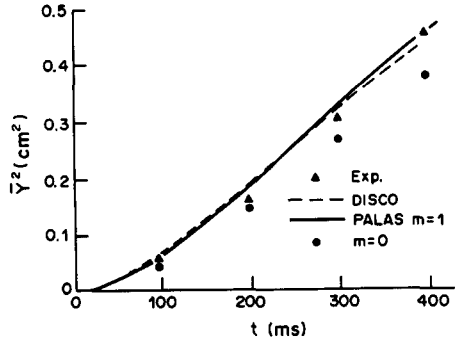


Figure 2. Fluid particle dispersion in turbulent pipe flow (Taylor & Middleman 1974).

Fluid particle trajectory simulation has been proved to be realistic and the next step in the description of the code PALAS on the discrete particle trajectory simulation is now presented.

## 3. DISCRETE PARTICLE TRAJECTORY

For a discrete particle, [1] does not apply due to the finite response time to changes in flow. The method to follow a discrete particle is therefore quite different from the scheme used previously for a fluid particle.

The simulation of a trajectory relies on the equation of motion of a particle. A modified Riley (1971) equation has been used, and is expressed as follows:

$$\rho_p v \frac{d\mathbf{V}}{dt} = -\frac{3}{4}\frac{v}{d}\rho_f C_D(\mathbf{V}-\mathbf{U})|\mathbf{V}-\mathbf{U}| - \rho_f v C_A \frac{d(\mathbf{V}-\mathbf{U})}{dt} + v(\rho_p-\rho_f)\mathbf{g} + \rho_f v \frac{D\mathbf{U}}{Dt} - \frac{3}{2d} v C_H \sqrt{\frac{\rho_f \mu}{\pi}} \int_{-\infty}^{t} \frac{\frac{d(\mathbf{V}-\mathbf{U})}{dt}}{(t-\tau)^{1/2}} d\tau, \quad [15]$$

where $\rho_p$ and $\rho_f$ are the particle and fluid density, respectively, $v$ is the particle volume, $\mathbf{V}$ and $\mathbf{U}$ are the instantaneous velocity of the particle and the fluid, respectively, $d$ is the particle diameter, $\mathbf{g}$ is the gravity vector, $d/dt$ is the temporal derivative along the discrete particle trajectory and $D/Dt$ is the temporal derivative along the fluid motion. The coefficients $C_D$, $C_H$ and $C_A$ are corrections which are introduced in the original Riley equation on the drag term, the history or Basset term and the added mass term, respectively, to take into account non-small particle Reynolds numbers and acceleration numbers. These coefficients are the only differences between the Riley equation and [15].

Equation [15] requires the following assumptions:

(i) The particles are spherical and undistorted.
(ii) The particles are not rotating.
(iii) The particles are not interacting and do not influence the turbulence.
(iv) Streamline curvature effects are neglected.

Let us also note that the particle diameter is assumed to be smaller than the Kolmogorov scale of the turbulence field, an assumption linked to the necessity to consider the fluid field as being quite homogeneous around the particle. However, this severe condition must be considered as sufficient but by no means necessary.

The particle Reynolds number is defined by

$$\mathrm{Re}_p = \frac{|\mathbf{V}-\mathbf{U}|d}{\nu}; \quad [16]$$

and, following Clift *et al.* (1978), for $\mathrm{Re}_p < 200$,

$$C_D = \frac{24}{\mathrm{Re}_p}(1 + 0.15\,\mathrm{Re}_p^{0.687}); \quad [17]$$

and, following Odar & Hamilton (1964), for $\mathrm{Re}_p < 60$,

$$C_A = 1.05 - \frac{0.066}{A_C^2 + 0.12}, \quad [18]$$

$$C_H = 2.88 + \frac{3.12}{(A_C+1)^3} \quad [19]$$

and

$$A_C = \frac{|\mathbf{V}-\mathbf{U}|^2}{d\left|\frac{d(\mathbf{V}-\mathbf{U})}{dt}\right|}. \quad [20]$$

For the comparisons described in the next section, the Basset term is neglected. This assumption has been justified by previous computations with the Eulerian approach. Equation [15] involves

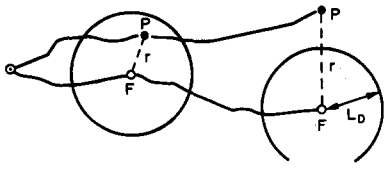


Figure 3. Fluid particle and discrete particle interaction.

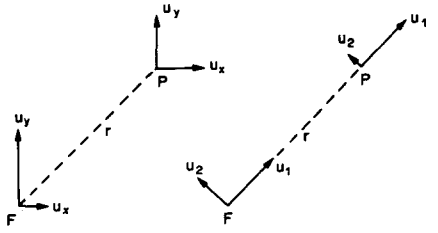


Figure 4. Change of the coordinate system.

instantaneous particle and fluid velocities. For the fluid, the instantaneous velocity is obtained by adding mean values from the turbulence data and a fluctuating contribution evaluated through the process described in subsection 2.1. We now mention that the temporal derivatives $\mathrm{d}/\mathrm{d}t$ and $\mathrm{D}/\mathrm{D}t$ of the fluid fluctuating velocities are neglected. Such a simplification is justified for low turbulence intensities and moderate departures from homogeneity (Ormancey 1984). The corresponding derivatives of fluid mean velocities are, however, preserved.

### *3.1. Integration of the Equation of Motion*

The main problem arising in the integration of the equation of motion of a discrete particle is to determine the instantaneous fluid velocity at the location of the discrete particle. The fluid mean velocity can be easily obtained by approximations of results from the $(K$–$\epsilon)$ model, but the fluctuating part of the velocity needs special treatment (Berlemont 1987; Desjonqueres 1987).

The method consists of the simultaneous simulation of a discrete and a fluid particle trajectory, starting from the same point at the same time. The fluid particle trajectory is constructed using the process previously described, and at each time step, it is required to determine the fluid velocity at the point P, where the discrete particle is, from the fluid velocity, known at point F, where the fluid particle is, as shown in figure 3. The "translation" from one point to another is carried out by use of Eulerian correlations. This requires a change in the coordinate system, so that the first base velocity $u_1$ is collinear to the vector **FP** (figure 4).

We then define a correlation matrix, which for two-dimensional cases reads

$$\begin{vmatrix} \overline{u_1^2(\mathrm{F})} & & & \\ \overline{u_1 u_2(\mathrm{F})} & \overline{u_2^2(\mathrm{F})} & & \\ \overline{u_1(\mathrm{F})u_1(\mathrm{P})} & \overline{u_2(\mathrm{F})u_1(\mathrm{P})} & \overline{u_1^2(\mathrm{P})} & \\ \overline{u_1(\mathrm{F})u_2(\mathrm{P})} & \overline{u_2(\mathrm{F})u_2(\mathrm{P})} & \overline{u_1(\mathrm{P})u_2(\mathrm{P})} & \overline{u_2^2(\mathrm{P})} \end{vmatrix}, \qquad [21]$$

where the correlations are expressed with the Frenkiel family of correlations, i.e.

$$\overline{u_i(\mathrm{F})u_j(\mathrm{P})} = \sqrt{\overline{u_i^2(\mathrm{F})}}\sqrt{\overline{u_j^2(\mathrm{P})}}\exp\left[\frac{-r}{(m^2+1)\mathrm{L}_{\mathrm{E}ij}}\right]\cos\left[\frac{mr}{(m^2+1)L_{\mathrm{E}ij}}\right], \qquad [22]$$

where $r$ is the distance between the points P and F and $\mathrm{L}_{\mathrm{E}ij}$ are Eulerian spatial correlation scales, which are known from experimental data or turbulence modelling. An inverse change of the coordinate system leads then to the required fluctuating velocites, $u_x$ and $u_y$ for example.

However, the distance between the points F and P must be significant for the correlation domain defined around the fluid particle. This means that if the discrete particle and the fluid particle are moving too far away from each other, the instantaneous fluid velocity "encountered" by the discrete particle can not be estimated by the scheme.

We are faced with the well-known phenomenon of crossing-trajectory effects, which is exhibited here. We thus define a length scale $L_{\mathrm{D}}$ which characterizes the correlation domain. When the discrete particle is outside that domain, i.e. when $r > L_{\mathrm{D}}$, we "change" the fluid particle. The trajectory of the new fluid particle is then simulated from the location of the discrete particle, and so on (figure 3). The whole process leads to a discrete particle trajectory Lagrangian simulation, and theoretically solves the problem.

However, it appears that an important problem lies in the scale computations. This problem concerns, more specifically, turbulence modelling and still remains unsatisfactorily solved. This is

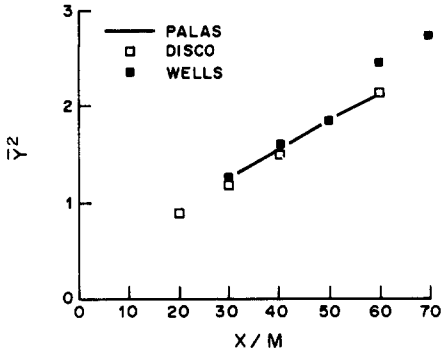


Figure 5. Crossing-trajectory effects in grid turbulence (Wells & Stock 1983), $E = -25{,}800$ V.

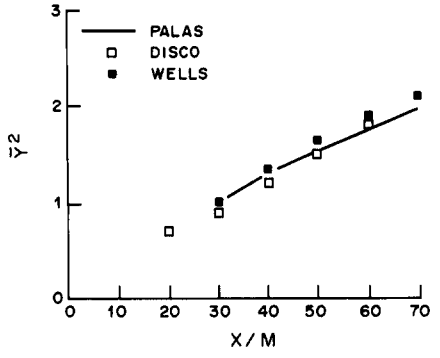


Figure 6. Crossing-trajectory effects in grid turbulence (Wells & Stock 1983), $E = 0$ V.

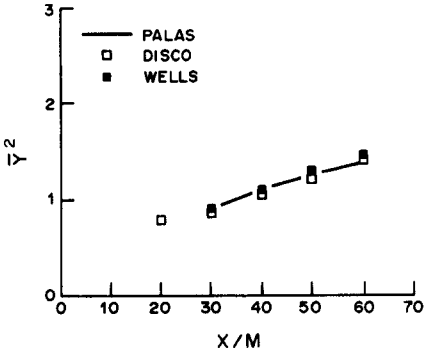


Figure 7. Crossing-trajectory effects in grid turbulence (Wells & Stock 1983), $E = 28{,}700$ V.

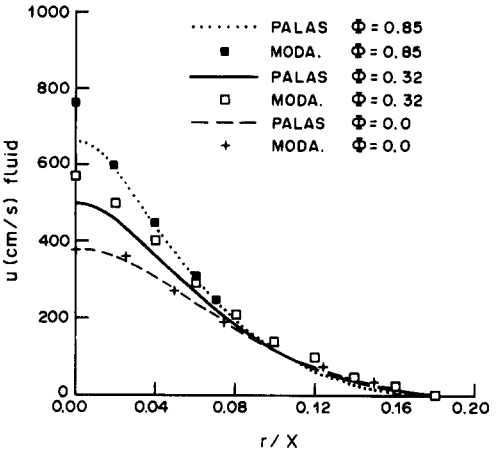


Figure 8. Jet case 1: fluid mean velocities (Modarress *et al.* 1984).

the reason why the validation of the dispersion module of the code PALAS has been carried out with experimental data for the scales, where possible. Otherwise, relations are defined as follows:

$$\tau_{L,ij} = C_L \frac{\overline{u_i u_j}}{\epsilon} \qquad [23a]$$

and

$$L_{Eij} = C_{ij} \sqrt{\overline{u_i u_j}}\, \tau_{Lij}, \qquad [23b]$$

where $C_{ij}$ is a constant depending on the scale considered. Let us note that for isotropic turbulence, $L_{E22} = L_{E11}/2$, when $L_{E11}$ is known, for instance. The constant $C_L$ is taken equal to 0.2 for jets or pipe flows (Picart *et al.* 1986). The correlation length scale $L_D$ is taken as an arithmetic mean value between the normal scales.

### *3.2. Comparisons with Experimental Results*

The Lagrangian approach has been compared with different experimental situations, namely the experiments of Snyder & Lumley (1971), Wells & Stock (1983) and Arnason (1982). The results of all these comparisons can be found in Desjonqueres (1987), Berlemont (1987) and Gouesbet *et al.* (1987), only the comparisons with the Wells & Stock (1983) experiments are presented here.

The experimental set-up consisted of a grid turbulence, and the main direction of the flow was horizontal. Turbulence measurements were made and energy decay laws characterizing the flow were given. These laws are used in the simulations to describe the turbulence field. The particles were glass spheres, with dia 5 or 57 $\mu$m and density = 2.45 g/cm$^3$. They were injected along the centre of the flow and submitted to electrical field $E$ to control the crossing-trajectory effects. These external forces tend to decrease or amplify the gravity forces.

Results are presented in figures 5–7 concerning the experimental data, Lagrangian simulations with the code PALAS and results from the Eulerian approach DISCO (Picart *et al.* 1986). The mean square displacement $\overline{Y^2}$ is plotted vs $X/M$, where $X$ is the distance from the beginning of the dispersion and $M$ is the grid mesh. Very good agreement is observed between all the results. Let us note that the agreement between DISCO (Eulerian approach) and PALAS (Lagrangian approach) is quite impressive. However, the simulation of the crossing-trajectory effects is much more physically realistic in the Lagrangian approach than in the Eulerian approach, where it is involved through a semi-empirical correction factor which contains a constant $C_\beta$. Let us mention that a wrong value for this constant has been stated previously (Picart *et al.* 1986). The new value is half the the proposed value, namely 0.42 instead of 0.85. The reason for the error was an incorrect translation of one FORTRAN statement, i.e. a constant $C'_\beta$ was used, which was equal to $2C_\beta$. All other results and discussions in Picart *et al.* (1986) are unmodified.

## 4. INFLUENCE OF THE PARTICLES ON THE TURBULENCE

In the above simulations, it was assumed that the particles do not modify significantly the turbulent structure of the flow field. But in many situations, the mass loading ratio is large enough to make this asssumption unrealistic. We, thus, have to use a two-way coupling scheme between turbulence and particles.

The scheme consists of momentum and energy exchanges between both phases (e.g. Durst *et al.* 1984; Shuen *et al.* 1985; Milojevic & Borner 1986). Iterations are carried out between the turbulence module and the particle module, which in the present studies are $<3$. Momentum exchanges between both phases occur through surface forces and are dependent on the particle volume fraction. Thus, the source term for the momentum equations reads

$$\overline{S_{pi}} = -\bar{\varepsilon}\rho_p\left[\left\langle\frac{dV_i}{dt}\right\rangle - g_i\left(1-\frac{\rho_f}{\rho_p}\right)\right], \qquad [24]$$

where $\bar{\varepsilon}$ is the temporal average value of the particle volume fraction, $\langle\ \rangle$ represents the set average over a number of particle trajectories and $V_i$ is the instantaneous particle velocity in the $i$th direction. It is assumed in such a relation that the ergodicity theorem is valid, meaning that temporal average and set average can be identified.

The approximation for each trajectory (over a large number of trajectories) reads

$$\frac{dV_i}{dt} = V_j^{av}\frac{V_i^o - V_i^i}{X_i^o - X_j^i}, \qquad [25]$$

where the superscript "o" stands for output and the superscript "i" for input of the $i$th cell (indicated by subscript $i$), $X_j$ is the $j$th coordinate and $V_j^{av}$ is the mean velocity of the particle in the cell.

The exact source term for the turbulence energy is (Desjonqueres 1987)

$$S_{pk} = \overline{u_i s_{pi}} = \overline{U_i S_{pi}} - \overline{U_i}\,\overline{S_{pi}}, \qquad [26]$$

where $u_i$ and $s_{pi}$ refer to instantaneous values.

The exact source term for the dissipation equation is

$$S_{p\varepsilon} = 2\nu\overline{\frac{\partial u_i}{\partial x_j}\frac{\partial s_{pi}}{\partial x_j}} \qquad [27]$$

which is modelled as

$$S_{p\varepsilon} = C_{\varepsilon 3}\frac{\epsilon}{K}S_{pk}, \qquad [28]$$

where $C_{\varepsilon 3}$ is a new constant.

### *4.1. Comparisons with Three Jets*

It is first important to mention that the results which are presented here have been obtained with the same code, without any change in the program, except the initial conditions, flow geometry and length or time steps.

The following constants were used, including the well-known corrections for a turbulent round jet (Launder & Spalding 1974):

*(K–ϵ) model*

$$C_\mu = 0.09 - 0.04f,$$

$$C_{\epsilon 2} = 1.92 - 0.067f$$

and

$$f = \left[\frac{Y}{2\Delta U}\left\langle \frac{\partial U_c}{\partial x} - \left|\frac{\partial U_c}{\partial x}\right| \right\rangle\right]^{0.2},$$

where $U_c$ is the longitudinal velocity on the jet axis, $Y$ is the half-width of the jet and $\Delta U$ is the radial variation of the velocity over $Y$;

$$C_1 = 1.44, \quad \sigma_K = 1.0, \quad \sigma_\epsilon = 1.3.$$

*Algebraic relations for $\overline{u_i u_j}$ (Rodi 1979; Gouesbet & Berlemont 1981)*

$$C_1' = 2.5, \quad \gamma_1 = 0.76, \quad \gamma_2 = 0.17, \quad \gamma_3 = 0.2.$$

*Particle/turbulence interaction*

$$C_{\epsilon 3} = 1.9.$$

Statistics are carried out for 5000 trajectories, which leads to a typical CPU time (IBM 3090) of 200 s, when the time step is equal to $\tau_L/10$. Statistical errors are very small as can be observed from the smooth character of the curves. Residual oscillations (as in, for example, figure 17) could be attenuated by increasing the number of trajectories.

### *4.1.1. Jet case 1 (Modarress et al. 1984)*

The first case concerns Modarress *et al.*'s (1984) experiment. A turbulent round free jet of air discharges from a pipe of $D = 2$ cm dia in an external air flow (dia = 60 cm) of very small velocity, meaning that it can be assumed to be at rest. Glass particles of 50 $\mu$m dia, with mass loadings of $\Phi = 0.32$ or 0.85 are transported by the flow. More details on the experimental design are given in table 1. The whole set of results is presented in Milojevic & Börner (1986) and only some of them are reported here. The fluid mean velocity is presented in figure 8, for $X/D = 20$, where $X$ is the distance from the jet exit, for $\Phi = 0$ (no particle), 0.32 and 0.85 vs $r/X$, where $r$ is the distance to the axis. The agreement is perfect for $\Phi = 0$, merely reflecting the quality of the turbulence model. The overall agreement between the simulations and experiments is very satisfactory for $\Phi = 0.32$ and 0.85, where the presence of particles increases the jet velocity. The particle velocities are shown in figure 9 for $\Phi = 0.32$ and 0.85. The agreement is again very satisfactory.

Figure 10 presents the fluid r.m.s. velocities for $X/D = 20$ and $\Phi = 0.32$, and figure 11 shows the cross-correlations $\overline{u_x u_r}$ for the same conditions. Again, all these comparisons are very satisfactory.

Table 1

| | |
|---|---|
| *Fluid phase* | |
| Centreline velocity (m/s) | 12.6 |
| Density (kg/m$^3$) | 1.178 |
| Mass flow rate (kg/s) | $3.76 \times 10^{-3}$ |
| Reynolds number | 13,300 |
| *Solid phase* | |
| Particle diameter ($\mu$m) | 50 |
| Particle density (kg/m$^3$) | 2990 |
| Centreline velocity (m/s) | 12.5 |
| Mass flow rate (kg/s) | |
| $\Phi = 0.32$ | $1.2 \times 10^{-3}$ |
| $\Phi = 0.85$ | $3.2 \times 10^{-3}$ |

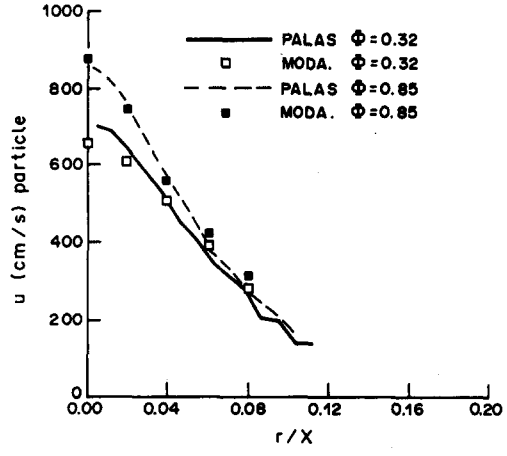


Figure 9. Jet case 1: particle mean velocities (Modarress *et al.* 1984).

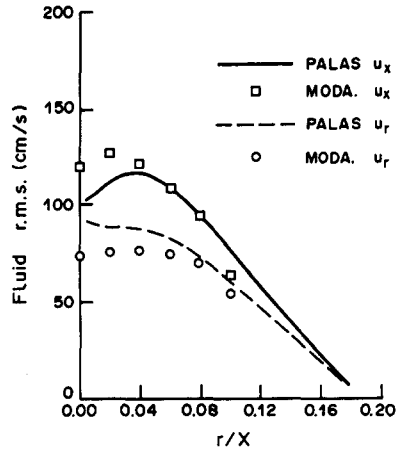


Figure 10. Jet case 1: fluid r.m.s. velocities (Modarress *et al.* 1984).

The particle r.m.s. velocity is shown in figure 12 for $\Phi = 0.32$ and $X/D = 20$. The experimental results are under-predicted, but the agreement is still satisfactory. Finally, the jet half-width is presented in figure 13 for $\Phi = 0.32$ and 0.85, and the simulations and the experimental data agree very well.

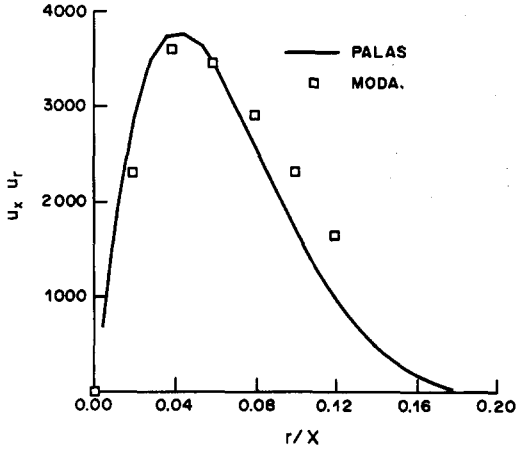


Figure 11. Jet case 1: fluid cross-correlation (Modarress *et al.* 1984).

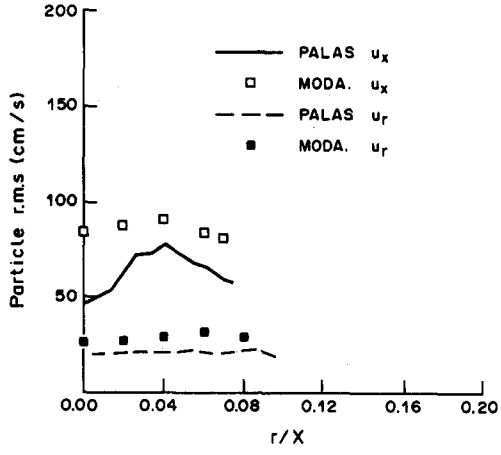


Figure 12. Jet case 1: particle r.m.s. velocities (Modarress *et al.* 1984).

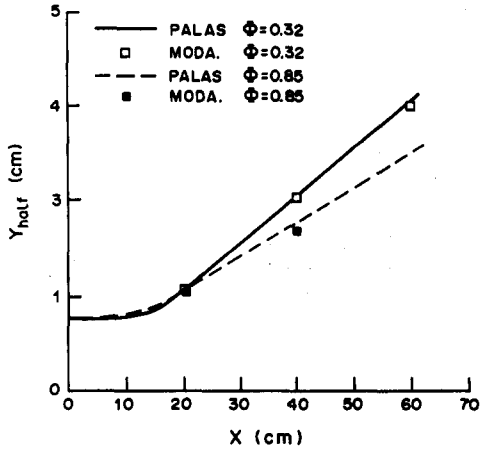


Figure 13. Jet case 1: jet half-width (Modarress *et al.* 1984).

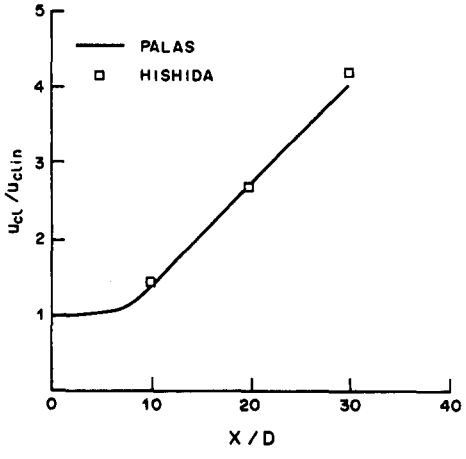


Figure 14. Jet case 2: centreline mean velocity (Hishida *et al.* 1985).

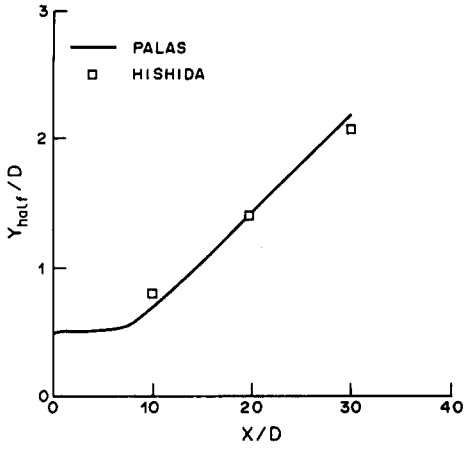


Figure 15. Jet case 2: jet half-width (Hishida *et al.* 1985).

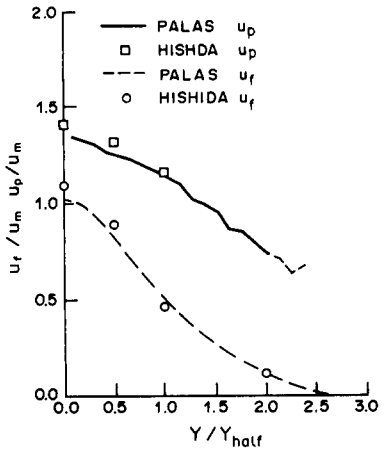


Figure 16. Jet case 2: fluid and particle mean velocities, $X/D = 10$ (Hishida *et al.* 1985).

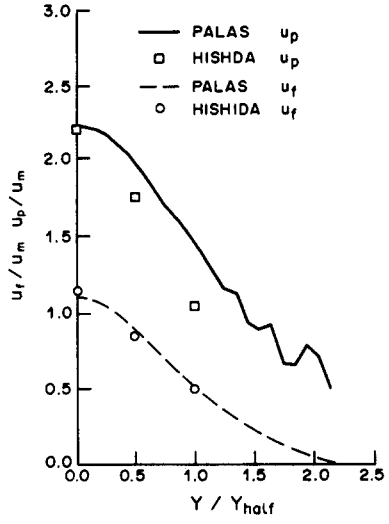


Figure 17. Jet case 2: fluid and particle mean velocities, $X/D = 20$ (Hishida *et al.* 1985).

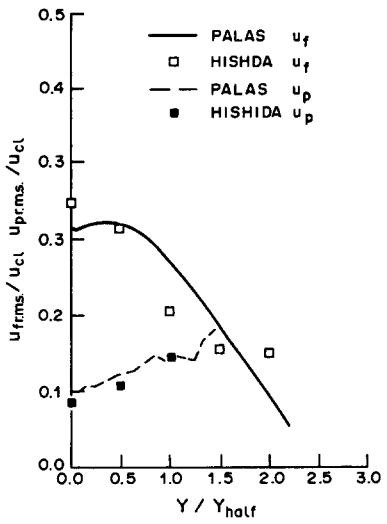


Figure 18. Jet case 2: fluid and particle r.m.s. velocities, $X/D = 20$ (Hishida *et al.* 1985).

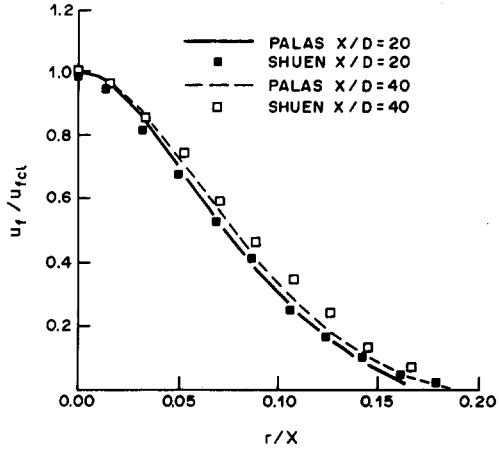


Figure 19. Jet case 3: fluid mean velocity (Shuen *et al.* 1985), $X/D = 20$ and $X/D = 40$.

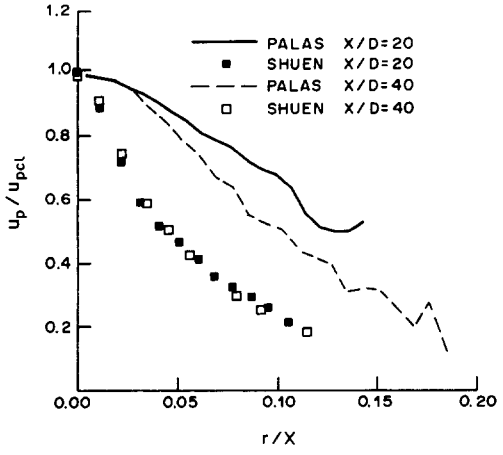


Figure 20. Jet case 3: particle mean velocity (Shuen *et al.* 1985), $X/D = 20$ and $X/D = 40$.

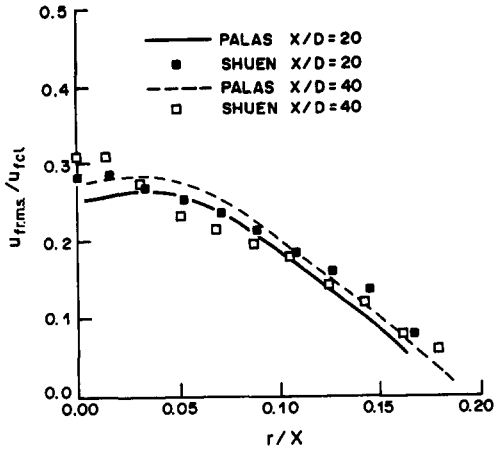


Figure 21. Jet case 3: fluid r.m.s. velocity (Shuen *et al.* 1985), $X/D = 20$ and $X/D = 40$.

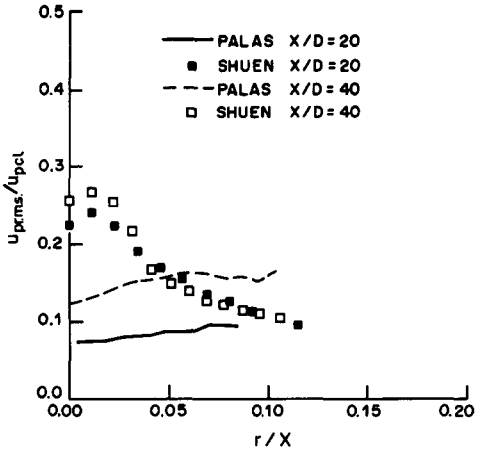


Figure 22. Jet case 3: particle r.m.s. velocity (Shuen *et al.* 1985), $X/D = 20$ and $X/D = 40$.

### *4.1.2. Jet case 2 (Hishida et al. 1985)*

The flow geometry consists of a 13 mm dia pipe which is discharging air at 30 m/s, loaded with glass particles of density 2.550 kg/m$^3$. The mass loading ratio is 0.3 and the Reynolds number is $2.2 \times 10^4$.

The fluid centreline mean velocity is presented in figure 14 and the jet half-width in figure 15, vs $X/D$. The agreement is very satisfactory.

The fluid and particle mean velocity profiles are presented in figures 16 and 17, for two locations, namely $X/D = 10$ and 20. $U_m$ is the mean centreline velocity for the single phase and $Y_{1/2}$ is the jet half-width. Very good agreement is observed for the fluid in both cases and for the particle at $X/D = 10$, but slight discrepancies are observed at $X/D = 20$.

The longitudinal fluid and particle r.m.s. velocity at $X/D = 20$ are shown in figure 18. Quite good agreement is observed here also.

### *4.1.3. Jet case 3 (Shuen et al. 1985)*

The flow geometry is similar to the previous jets, but the particle mean diameter is 79 $\mu$m, the pipe diameter is 10.9 mm, the mean velocity is 24.1 m/s and the mass loading is 0.2 for particles with a density of 2.650 kg/m$^3$.

All the results are given vs the reduced radial coordinate $r/X$, and for two locations, namely $X/D = 20$ and 40. Fluid mean velocities are presented in figure 19 and particle mean velocities in

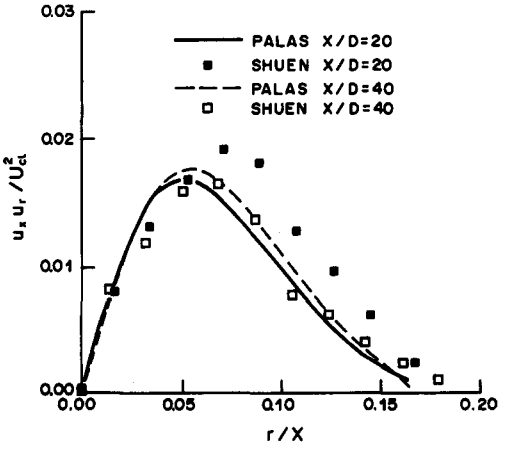


Figure 23. Jet case 3: fluid cross-correlation (Shuen *et al.* 1985), $X/D = 20$ and $X/D = 40$.

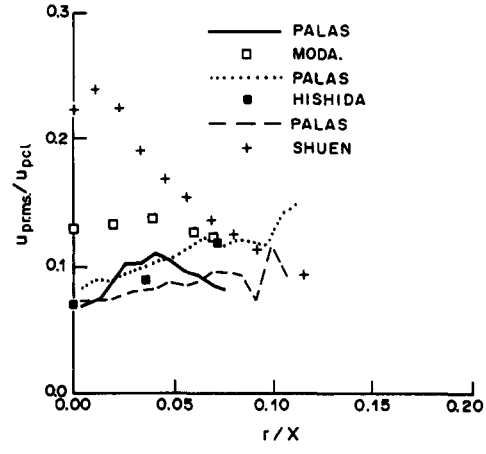


Figure 24. Comparison of particle r.m.s. velocities for the three jets, at $X/D = 20$.

figure 20. In the same way, the fluid and particle longitudinal r.m.s. velocity are plotted in figures 21 and 22. The tangential correlation $\overline{u_x u_r}$ is compared with experimental data in figure 23.

Good agreement is observed for the whole set of fluid results, as was previously noted. Some differences arise between predictions and experimental results for the particles, but as mentioned below, the initial conditions are probably the main reason for these discrepancies.

## 5. MISCELLANEOUS REMARKS

The initial conditions are obtained for the three cases by the same process. We assume fully-developed pipe flow profiles for the inlet conditions for the fluid. These results are obtained with a $(K-\epsilon)$ model, supplemented with algebraic relations for the Reynolds stress tensor. The inlet particle mean velocity is given in the experiment descriptions, and the particle fluctuating velocities are assumed to be equal to the fluid fluctuating velocities, quite a rough assumption due to the lack of precise experimental data.

It can be stated, obviously, that these initial conditions are probably not the exact experimental conditions, and they certainly produce some "undesired" errors in the predictions.

Since the three jets are quite identical, and to reflect experimental differences, figure 24 presents the particle fluctuating velocity profiles for the three jets and the three simulations. The particle r.m.s. velocity is reduced by the particle mean velocity and represented vs $r/X$, for the location $X/D = 20$.

It can be observed that the simulations are essentially identical for the three cases, while the experimental results exhibit a spreading behaviour. This shows both the difficulties in experimental studies and the importance of precise boundary and initial conditions in any simulation.

## 6. CONCLUSION

The Lagrangian approach which has been presented relies on particle trajectory simulations. The influence of turbulence on the particle behaviour is described by the simultaneous construction of two trajectories, one for a fluid particle and one for a discrete particle. The differences between the two trajectories are represented through Eulerian correlations which transfer information from the fluid to the particle.

For a fluid particle, we introduce a correlation matrix which evolves with the statistical properties of the flow encountered by the particle. A discrete particle trajectory is obtained with the aid of an equation of motion and taking into account the crossing-trajectory effects by a change in the fluid particle which is simultaneously followed.

The influence of the particles on the turbulence field is represented by the use of source terms in the governing equation of a $(K-\epsilon)$ model. These source terms are estimated from momentum and energy exchanges between both phases.

The code PALAS is compared with theoretical and experimental results, more particularly with:

—Fluid particle diffusion in homogeneous and isotropic turbulence (Hinze 1975).
—Fluid particle diffusion in a turbulent pipe flow (Taylor & Middleman 1974).
—Particle dispersion in grid turbulence (Wells & Stock 1983).
—Three two-phase turbulent particle-laden jets (Modarress *et al.* 1984; Hishida *et al.* 1985; Shuen *et al.* 1985).

The predictions compared favourably with the whole set of data and further developments of the code are now planned.

## REFERENCES

ABBAS, A. S., KOUSSA, S. S. & LOCKWOOD, F. C. 1980 The prediction of particle laden gas flow. Report FS/80/1, ICST, London.

ARNASON, G. 1982 Measurements of particle dispersion in turbulent pipe flow. Ph.D. Thesis, Washington State Univ., Pullman, Wash.

BERLEMONT, A. 1987 Modelisation Eulerienne et Lagrangienne de la dispersion particulaire en écoulement turbulent. These de Doctorat d'Etat, Rouen.

BERLEMONT, A., PICART, A. & GOUESBET, G. 1986 Prediction of turbulence fields and particle dispersion using the code DISCO-2. In *Computational Techniques for Fluid Flow*, Chap. 10, pp. 281–313. Pineridge Press, Swansea, U.K.

CIARLET, P. G. 1982 *Introduction à l'Analyse Numérique Matricielle.* Masson, Paris.

CLIFT, R., GRACE, J. R. & WEBER, M. E. 1978 *Bubbles, Drops and Particles.* Academic Press, New York.

DESJONQUERES, P. 1987 Modélisation Lagrangienne du comportement de particules discrètes en écoulement turbulent. Thèse de 3ème cycle, Rouen.

DESJONQUERES, P., GOUESBET, G., BERLEMONT, A. & PICART, A. 1986 Dispersion of discrete particles by continuous turbulent motions: new results and discussions. *Phys. Fluids* **29,** 2147–2151.

DURST, F., MILOJEVIC, D. & SCHONUNG, B. 1984 Eulerian and Lagrangian predictions of particulate two-phase flows: a numerical study. *Appl. math. Modelling* **8,** 101–115.

ELGHOBASHI, S. E., ABOU ARAB, T. W., RIZK, M. & MOSTAFA, A. 1984 Prediction of the particle laden jet with a two equation turbulence model. *Int. J. Multiphase Flow* **10,** 697–710.

FRENKIEL, F. N., 1948 Etude statistique de la turbulence—fonctions spectrales et coefficients de corrélation. Rapport Technique, ONERA No. 34.

GOSMAN, A. D. & IOANNIDES, E. 1981 Aspects of computer simulation of liquid-fuelled combustors. Presented at the *AAIA 19th Aerospace Science Mtg*, St Louis, Mo., Paper 81-0323.

GOUESBET, G. & BERLEMONT, A. 1981 Prediction of turbulent fields, including fluctuating velocity correlations and approximate spectra, by means of a simplified second order closure scheme: the round free jet and developed pipe flow. In *Proc. 2nd Int. Conf. on Numerical Methods in Laminar and Turbulent Flow, Venice, Italy*, pp. 205–216. Pineridge Press, Swansea, U.K.

GOUESBET, G., BERLEMONT, A. & PICART, A. 1984 Dispersion of discrete particles by turbulent continuous motions. Extensive discussion of Tchen's theory using a two parameter family of Lagrangian correlation functions. *Phys. Fluid* **27,** 827–837.

GOUESBET, G., DESJONQUERES, P. & BERLEMONT, A. 1987 Eulerian and Lagrangian approaches to turbulent dispersion of particles. Presented at the *ICHMT Semin. on Transient Phenomena in Multiphase Flow, Dubrovnic*, pp. 247–271. Hemisphere, Washington, D.C.

HINZE, J. O. 1975 *Turbulence.* McGraw-Hill, New York.

HISHIDA, K., KAENEKO, K. & MAEDA, M. 1985 Turbulence structure of a gas–solid two phase circular jet. *Trans. JSME Ser. B* **51,** 2330–2337.

LAUNDER, B. E. & SPALDING, D. B. 1974 The numerical computation of turbulent flows. *Comput. Meth. appl. Mech. Engng* **3,** 269.

MILOJEVIC, D. & BÖRNER, TH. 1986 Results on test case predictions. In *Proc. 3rd Wkshp on Two-phase Flow Predictions*, Belgrade, pp. 33–41.

MODARRESS, D., TAN, H. & ELGOBASHI, S. 1984 Two-component LDA measurement in a two-phase turbulent jet. *AIAA Jl* **22,** 624.

ODAR, F. & HAMILTON, W. S. 1964 Forces on a sphere acceleration in a viscous fluid. *J. Fluid Mech.* **18,** 302–314.

ORMANCEY, A. 1984 Simulation du comportement de particule dans des écoulements turbulents. Thèse de 3eme cycle, Ecole des Mines de Paris.

ORMANCEY, A. & MARTINON, A. 1984 Prediction of particle dispersion in turbulent flows. *Physico-Chem. Hydrodynam.* **5,** 229–240.

PICART, A. 1984 Le code DISCO-2 pour la prédiction du comportement de particules dans un ecoulement turbulent. Thèse de 3ème cycle, Rouen.

PICART, A., BERLEMONT, A. & GOUESBET, G. 1986 Modelling and predicting turbulence fields and the dispersion of discrete particles transported by turbulent flows. *Int. J. Multiphase Flow* **12,** 237–261.

REEKS, M. W. 1977 On the dispersion of small particle suspended in an isotropic turbulent fluid. *J. Fluid Mech.* **83,** 529–546.

RILEY, J. J. 1971 Ph.D. Thesis, The Johns Hopkins Univ., Baltimore, Md.

RODI, W. 1979 Turbulence models for environmental problems. *V.K.I. Lect. Ser. 2979-2.*

SHUEN, J. S., SOLOMON, A. S. P., ZHANG, Q. F. & FAETH, G. M. 1985 Structure of particle-laden jets: measurements and predictions. Report AIAA-84-0038.

SNYDER, W. H. & LUMLEY, J. L. 1971 Some measurements of particle velocity autocorrelation functions in a turbulent flow. *J. Fluid Mech.* **48,** 41–71.

TAYLOR, A. R. & MIDDLEMAN, S. 1974 Turbulent dispersion in drag-reducing fluids. *AIChE Jl* **20,** 454–461.

WELLS, M. R. & STOCK, D. E. 1983 The effects of crossing trajectories on the dispersion of particles in a turbulent flow. *J. Fluid Mech.* **136,** 31–36.

## APPENDIX

*Correlation Matrix for Two-dimensional Fluid Particle Trajectory Simulation*

$$
\begin{array}{c|cccccc}
 & \overline{u_x u_x(t)} & \overline{u_x u_y(t)} & \overline{u_x(t)u_x(t+\Delta t)} & \overline{u_x(t)u_y(t+\Delta t)} & \overline{u_x(t)u_x(t+2\Delta t)} & \overline{u_x(t)u_y(t+2\Delta t)} \\
\overline{u_x u_x(t)} & & & \overline{u_x u_x(t+\Delta t)} & \overline{u_x u_y(t+\Delta t)} & \overline{u_x(t+\Delta t)u_x(t+2\Delta t)} & \overline{u_x(t+\Delta t)u_y(t+2\Delta t)} \\
\overline{u_x u_y(t)} & & \overline{u_y u_y(t)} & \overline{u_y(t)u_x(t+\Delta t)} & \overline{u_y(t)u_y(t+\Delta t)} & \overline{u_y(t)u_x(t+2\Delta t)} & \overline{u_y(t)u_y(t+2\Delta t)} \\
\overline{u_x(t)u_x(t+\Delta t)} & & & & \overline{u_y u_y(t+\Delta t)} & \overline{u_y(t+\Delta t)u_x(t+2\Delta t)} & \overline{u_y(t+\Delta t)u_y(t+2\Delta t)} \\
\overline{u_x(t)u_y(t+\Delta t)} & & & & & \overline{u_x u_x(t+2\Delta t)} & \overline{u_x u_y(t+2\Delta t)} \\
\overline{u_x(t)u_x(t+2\Delta t)} & & & & & & \overline{u_y u_y(t+2\Delta t)} \\
\overline{u_x(t)u_y(t+2\Delta t)} & & & & & &
\end{array}
$$